Detection and Characterization of an Oxomanganese(V) Porphyrin Complex by Rapid-Mixing Stopped-Flow Spectrophotometry

John T. Groves,* Jinbo Lee, and Sudhakar S. Marla

Contribution from the Department of Chemistry, Princeton University, Princeton, New Jersey 08544

Received July 29, 1996. Revised Manuscript Received March 26, 1997[⊗]

Abstract: The first detection and characterization of oxomanganese(V) porphyrin complexes under ambient catalytic conditions is described. The reaction of (tetra-(*N*-methylpyridyl)porphyrinato)manganese(III) [Mn(III)TMPyP] with a variety of oxidants such as *m*-chloroperoxybenzoic acid (*m*-CPBA), HSO_5^-, and ClO^- has been shown to produce the same, short-lived intermediate (**1**) by stopped-flow spectrophotometry. The Soret maximum of **1** was found at 443 nm, intermediate between that of oxomanganese(IV) (428 nm) and Mn(III)TMPyP (462 nm), thus facilitating its detection. The rate of formation of **1** from Mn(III)TMPyP followed second-order kinetics, first order in Mn(III) porphyrin and first order in oxidant. The rate constants have the following order: *m*-CPBA (2.7×10^7 M^{-1} s^{-1}) > HSO_5^- (6.9×10^5 M^{-1} s^{-1}) ≈ ClO^- (6.3×10^5 M^{-1} s^{-1}). Once formed, the intermediate species **1** was rapidly converted to oxoMn(IV) (**2**) by one-electron reduction with a first-order rate constant of 5.7 s^{-1}. The oxoMn(IV) species **2** was relatively stable under the reaction conditions, decaying slowly to Mn(III)TMPyP with a first-order rate constant of 0.027 s^{-1}. The identity of **1** as an oxomanganese(V) complex was indicated by its reactivity. The one-electron reduction of **1** to oxoMn(IV) was greatly accelerated by nitrite ion ($k = 1.5 \times 10^7$ M^{-1} s^{-1}). However, the reaction between nitrite and oxoMn(IV) is much slower ($k = 1.4 \times 10^2$ M^{-1} s^{-1}). The oxoMn(V) intermediate **1** was shown to be highly reactive toward olefins, affording epoxide products. By contrast, oxoMn(IV) (**2**) was not capable of effecting the same reaction under these conditions. In the presence of carbamazepine (**3**) efficient oxygen transfer from the highly reactive oxoMn(V) (**1**) to the olefin (second-order rate constant of 6.5×10^5 M^{-1} s^{-1}) resulted in the conversion of **1** directly back to Mn(III)TMPyP without the appearance of the stable oxoMn(IV) intermediate **2**. With *m*-CPBA as the oxidant in the presence of $H_2{}^{18}O$, the product epoxide was shown to contain 35% ^{18}O, consistent with an O-exchange-labile oxoMn(V) intermediate. Nitrite ion inhibited the epoxidation reaction competitively by one electron reduction of the oxoMn(V) intermediate to the unreactive oxoMn(IV).

Introduction

Reactive metal−oxo intermediates are central to the mechanisms of an increasing family of biological and catalytic processes involving oxygen activation and transfer.[1−3] The most famous biochemical example is compound I of horseradish peroxidase, which has been characterized as an oxoiron(IV) porphyrin cation radical.[4] An oxomanganese(IV) protein radical species has been identified for manganese HRP.[5] High-valent oxometalloporphyrin complexes play an important role in a variety of reactions catalyzed by cytochrome P450,[2] chloroperoxidase,[6] and nitric oxide synthase (NOS),[7] and heme iron−oxo intermediates have been identified during the oxygen reduction cycle of cytochrome oxidase.[8]

Model studies using synthetic metalloporphyrins[5] have been fruitful in affording insights into the nature of these enzymatic processes.[2] Furthermore, these metalloporphyrin complexes have shown promise as process catalysts.[2a,9] While reactive oxometalloporphyrin complexes of chromium,[10a] iron,[10b,i] and ruthenium[10c,d] have been isolated and characterized, the corre-

* Author to whom correspondence should be addressed.

[⊗] Abstract published in *Advance ACS Abstracts,* June 15, 1997.

(1) (a) Sheldon, R. A.; Kochi, J. K. *Metal Catalyzed Oxidations of Organic Compounds*; Academic Press: New York, 1981. (b) *Activation and functionalization of alkanes*; Hill, C. L., Ed.; John Wiley & Sons: New York, 1989.

(2) (a) Groves, J. T.; Han, Y.-Z. In *Cytochrome P-450. Structure, Mechanism and Biochemistry*; Ortiz de Montellano, P. R., Ed.; Plenum Press: New York, 1995; pp 3−48. (b) *Selective Hydrocarbon Activation: Principle and Progress*; Davies, J. A., et al., Eds.; VCH: New York, 1994.

(3) (a) *Metalloporphyrins in Catalytic Oxidations*; Sheldon, R. A., Ed.; Marcel Dekker: New York, 1994. (b) Mlodnika, T.; James, B. R. In *Metalloporphyrin Catalyzed Oxidations*; Montanari, F., Casella, L., Eds.; Kluwer: Dordrecht, The Netherlands, 1994; p 121.

(4) (a) Mann, T. In *Oxidases and Related Redox Systems*; King, T. E., Mason, H. S., Morrison, M., Eds.; Liss: New York, 1988; pp 29−49. (b) Dolphin, D.; Forman, A.; Borg, D. C.; Fayer, J.; Felton, R. H. *Proc. Natl. Acad. Sci. U.S.A.* **1971**, *68*, 614−618. (c) Dolphin, D.; Felton, R. H. *Acc. Chem. Res.* **1974**, *7*, 26−32. (d) Peisach, J.; Blumberg, W. E.; Wittenberg, B. A.; Wittenberg, J. B. *J. Biol. Chem.* **1968**, *243*, 1871−1880. (e) Penner-Hahn, J. E.; McMurry, T. J.; Renner, M.; Latos-Grazynsky, L.; Eble, K. S.; Davis, I. M.; Balch, A. L.; Groves, J. T.; Dawson, J. R.; Hodgson, K. O. *J. Biol. Chem.* **1983**, *258*, 12761−12764.

(5) Nick, R. J.; Ray, G. B.; Fish, K. M.; Spiro, T. G.; Groves, J. T. *J. Am. Chem. Soc.* **1991**, *113*, 1838−1840.

(6) Fann, Y.-C.; Gerber, N. C.; Osmulski, P. A.; Hager, L. P.; Sligar, S. G.; Hoffmann, B. M. *J. Am.Chem. Soc.* **1994**, *116*, 5989−5990.

(7) (a) Marletta, M. A. *J. Biol. Chem.* **1993**, *268*, 12231. (b) White, K. A.; Marletta, M. A. *Biochemistry* **1992**, *31*, 6627. (c) McMillan, K.; Bredt, D. S.; Hirsch, D. J.; Snyder, S. H.; Clark, J. E.; Masters, B. S. S. *Proc. Natl. Acad. Sci. U.S.A.* **1992**, *89*, 1141−1145.

(8) (a) Varotsis, C.; Zhang, Y.; Appleman, E. H.; Babcock, G. T. *Proc. Natl. Acad. Sci. U.S.A.* **1993**, *90*, 237−241. (b) Ogura, T.; Hirota, S.; Proshlyakov, D. A.; Shinzawa-Itoh, K.; Yoshikawa, S.; Kitagawa, T. *J. Am. Chem. Soc.* **1996**, *118*, 5443−5449.

(9) (a) *Metalloporphyrins in Catalytic Oxidations*; Sheldon, R. A., Ed.; Marcel Dekker: New York, 1994. (b) Ellis, P. E.; Lyons, J. E. *Coord. Chem. Rev.* **1990**, *105*, 181−193.

(10) (a) Groves, J. T.; Kruper, W. J. *J. Am. Chem. Soc.* **1979**, *101*, 7613−7614. (b) Groves, J. T.; Haushalter, R. C.; Nakamura, M.; Nemo, T. E.; Evans, B. J. *J. Am. Chem. Soc.* **1981**, *102*, 2884−2886. (c) Groves, J. T.; Quinn, R. *Inorg. Chem.* **1984**, *23*, 3844−3846. (d) Groves, J. T.; Quinn, R. *J. Am. Chem. Soc.* **1985**, *107*, 5790−5792. (e) Groves, J. T.; Watanabe, Y.; McMurry, T. J. *J. Am. Chem. Soc.* **1983**, *105*, 4489−4490. (f) Groves, J. T.; Stern, M. K. *J. Am. Chem. Soc.* **1988**, *110*, 8628−8638. (g) Czernuszewicz, R. S.; Su, Y. O.; Stern, M. K.; Macor, K. A.; Kim, D.; Groves, J. T.; Spiro, T. G. *J. Am. Chem. Soc.* **1988**, *110*, 4158−4165. (h) Groves, J. T.; Watanabe, Y. *Inorg. Chem.* **1986**, *25*, 4808. (i) Groves, J. T.; Watanabe, Y. *J. Am. Chem. Soc.* **1988**, *110*, 8443−8452.

S0002-7863(96)02605-4 CCC: $14.00

sponding oxomanganese(V) species have proven to be particularly elusive.[10e,f] By contrast, nitridomanganese(V) porphyrins have been well characterized.[11] These complexes are stable and inert toward typical substrates, although N-acylation produced a reactive nitrene transfer agent.[12] Stable oxomanganese(V) complexes are few, the only examples involving the use of tetraanionic ligands to stabilize the high-valent manganese center.[13,14] The intermediacy of reactive oxomanganese(V) porphyrin complexes has long been implicated from reactivity patterns and ^{18}O-exchange into products from water,[10e,f,h,15,16] and relatively stable oxomanganese(IV) porphyrin intermediates have been isolated and well characterized.[10f,g]

Here we describe the first detection of a reactive oxomanganese(V) intermediate under ambient reaction conditions by rapid-mixing stopped-flow techniques and a direct assessment of its reactivity in both one-electron and oxygen transfer processes.

Results and Discussion

The reaction of (tetra-*N*-(methylpyridyl)porphyrinato)manganese(III) (Mn(III)TMPyP) with *m*-chloroperoxybenzoic acid (*m*-CPBA) in 50 mM pH 7.4 phosphate buffer was analyzed by stopped-flow spectrophotometry at 25 °C. The UV−vis spectra obtained upon mixing 5 μM solutions of each reactant are shown in Figure 1. As can be seen, the starting manganese(III) porphyrin spectrum (462 nm) was completely transformed within 30 ms into that of a new intermediate (**1**) with a strong and relatively sharp Soret maximum at 443 nm. In a slower, subsequent phase of the reaction, the spectrum of **1** was replaced by **2**, which has the signature spectrum of an oxomanganese(IV) porphyrin.[10f,g,11,13] Kinetic analysis of the data indicates a second-order rate for the formation of **1**, $k_1 = 2.7 \times 10^7$ M^{-1} s^{-1}, and a first-order decay of **1** to afford **2**, $k_2 = 5.7$ s^{-1}.[17]

The nature of **1** could be deduced by analysis of its reactions with reducing substrates. Thus, the generation of **1** in the presence of 1 equiv of nitrite ion greatly accelerated the conversion of **1** to **2**, a one-electron reduction. In the presence of 10 equiv of nitrite, intermediate **1** was no longer observable and the direct formation of oxoMn(IV) from Mn(III) was apparent with clear isosbestic points at 447 and 389 nm (Figure 2a). The reduction of **1** by nitrite under pseudo-first-order conditions was so fast that it was impossible to collect the full kinetic time course using the stopped-flow instrument. However, the second-order rate constant for the reaction of nitrite with **1** could be estimated to be 1.5×10^7 M^{-1} s^{-1} using second-order kinetic analysis in a double-mixing experiment (Figure 3a), in which **1** was produced in the first mixing and subsequently mixed with nitrite after 22 ms. Interestingly, the second reduction of **2** by nitrite back to the starting manganese(III) porphyrin was quite slow under these conditions with a rate constant of 1.4×10^2 M^{-1} s^{-1} (Figure 3b).

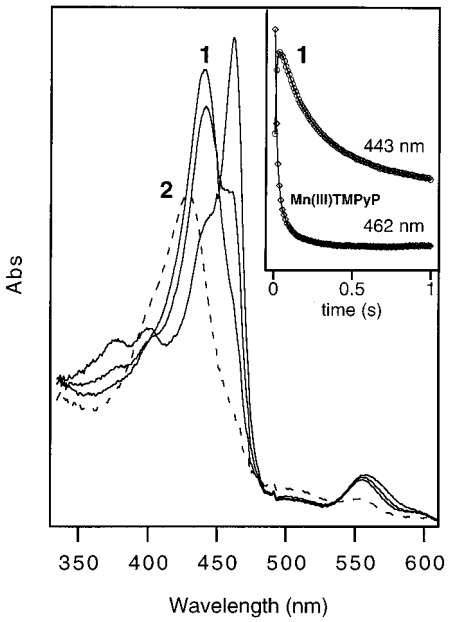

Figure 1. Time-resolved UV−vis spectra for the stoichiometric reaction between 5 μM Mn(III)TMPyP and 5 μM *m*-CPBA (100 scans in 1 s, 0.005 s integration time for the photodiode array; full ordinate scale 0.35 OD). The accumulation of intermediate **1** is represented in the three solid traces (spectra at 0, 0.01, and 0.03 s). Intermediate **1** subsequently decays to **2**; the spectrum of **2** is shown as the dotted trace (spectrum at 1 s). Inset (full ordinate scale 0.30 OD): kinetic profiles for **1** monitored at 443 nm (upper trace) and for Mn(III)TMPyP at 462 nm (lower trace) from the same data set.

The reaction of Mn(III)TMPyP with *m*-CPBA in the presence of an olefin substrate, carbamazepine (5*H*-dibenzo[*b*,*f*]azepine-5-carboxamide) **3**, led to the formation of epoxide in good yield (93%).[18] Significantly, the formation of **1** in the presence of 10 equiv of **3** greatly suppressed the formation of the oxoMn(IV) species **2** and diverted the reaction to reform the starting Mn(III) complex (Figure 2b). In the absence of olefin substrate, the intermediate **1** monitored at 443 nm was fully formed and subsequently decayed to oxoMn(IV) (**2**, Figure 1, inset). The same process monitored at the Mn(III) Soret (462 nm) revealed a sharp decrease in absorbance during the formation of **1**, but the absorbance remained unchanged as **1** was converted to **2** (Figure 1, inset). On the other hand, totally different kinetic profiles were obtained from the double-mixing experiments in which **1** was fully formed during the first mixing step by reacting 5 μM Mn(III)TMPyP with 5 μM *m*-CPBA and then CBZ was added in the second mixing step under pseudo-first-order conditions. The intermediate **1**, monitored at 443 nm, decayed quickly due to the epoxidation of **3**, accompanied by concurrent recovery of Mn(III) monitored at 462 nm (Figure 4a). The second-order rate of reaction of **1** to afford epoxide and Mn-

(11) (a) Buchler, J. W.; Dreher, C.; Lay, K. L.; Lee, Y. J. A.; Scheidt, W. R. *Inorg. Chem.* **1983**, *22*, 888−891. (b) Hill, C. L.; Hollander, F. J. *J. Am. Chem. Soc.* **1982**, *104*, 7318−7319.

(12) (a) Groves, J. T.; Takahashi, T. *J. Am. Chem. Soc.* **1983**, *105*, 2073−2074. (b) Bottomley, L. A.; Neely, F. L. *J. Am. Chem. Soc.* **1988**, *110*, 6748−6752. (c) Bottomley, L. A.; Neely, F. L. *J. Am. Chem. Soc.* **1989**, *111*, 5955−5957. (d) Woo, L. K.; Goll, G. G.; Czapla, D. J.; Hays, J. A. *J. Am. Chem. Soc.* **1991**, *113*, 8478−8484.

(13) (a) Collins, T. J.; Gordon-Wylie, S. W. *J. Am. Chem. Soc.* **1989**, *111*, 4511−4513. (b) Collins, T. J.; Powell, R. D.; Slebodnick, C.; Uffelman, E. S. *J. Am. Chem. Soc.* **1990**, *112*, *899*−901.

(14) MacDonnell, F. M.; Fackler, N. L. P.; Stern, C.; O'Halloran, T. V. *J. Am. Chem. Soc.* **1994**, *116*, 7431−7432.

(15) Groves, J. T.; Marla, S. S. *J. Am. Chem. Soc.* **1995**, *117*, 9578−9579.

(16) (a) Bernadou, J.; Fabiano, A. S.; Robert, A.; Meunier, B. *J. Am. Chem. Soc.* **1994**, *116*, 9375−9376. (b) Pitie, M.; Bernadou, J.; Meunier, B. *J. Am. Chem. Soc.* **1995**, *117*, 2935−2936.

(17) Kinetic profiles of the stoichiometric reaction between 5 μM Mn(III)TMPyP and 5 μM *m*-CPBA were monitored at 443 and 462 nm. The formation of **1** was analyzed as a homogeneous second-order reaction. Both linear least-squares fitting of $(A_0 - A_\infty)/(A - A_\infty)$ vs time ($R = 0.9990$) and nonlinear least-squares fitting of the kinetic profile ($R = 0.9982$) give a second-order rate constant of 2.7×10^7 M^{-1} s^{-1}. The decay of **1** to **2** is a first-order process with an excellent fit into a single exponential ($k = 5.7$ s^{-1}; $R = 0.9999$). On the basis of these rate constants, the full kinetic profiles were nicely simulated globally using HopKINSIM simulation program.

(18) Into a reaction mixture of 50 μM Mn(III)TMPyP and 520 μM carbamazepine (CBZ) in 50 mM pH 7.4 phosphate buffer, 300 μM of *m*-CPBA was added in six aliquots of 50 μM each at 2 min intervals. Quantitative analyses of the reaction products were performed by HPLC. (Detailed reaction conditions and analyses are available in Experimental Section.) Under these conditons, the conversion (based on oxidant consumed) of the olefin was 35% and the yield of epoxide was 93%. In the presence of 600 μM of nitrite ion, less than 3% of the epoxide was found.

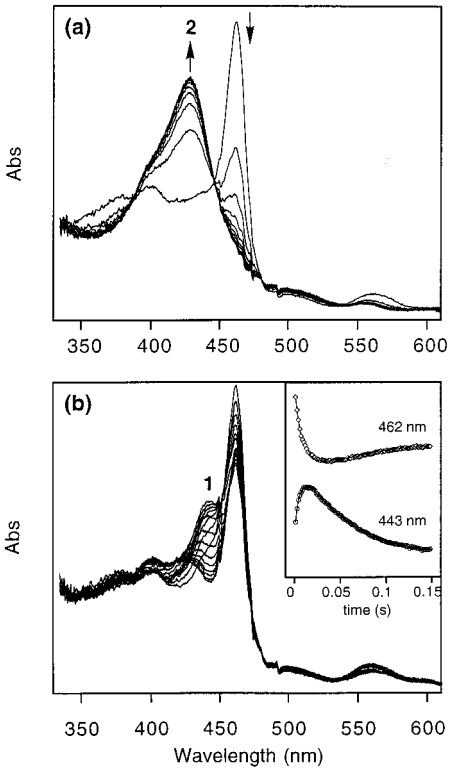

Figure 2. Time-resolved UV−vis spectra for the reaction of 5 μM Mn(III)TMPyP and 5 μM *m*-CPBA, (a) in the presence of 50 μM $NaNO_2$ (100 scans in 150 ms, 0.0015 s integration time for the photodiode array; full ordinate scale 0.40 OD; every tenth scan shown) and (b) in the presence of 50 μM carbamazepine (100 scans in 150 ms, 0.0015 s integration time for the photodiode array; full ordinate scale 0.40 OD; spectra at 0−6 ms show partial accumulation of **1**; spectra at 15−150 ms show conversion of **1** directly back to Mn(III)-TMPyP). Inset (full ordinate scale 0.32 OD): kinetic profiles for **1** monitored at 443 nm (lower trace) and for Mn(III)TMPyP at 462 nm (upper trace).

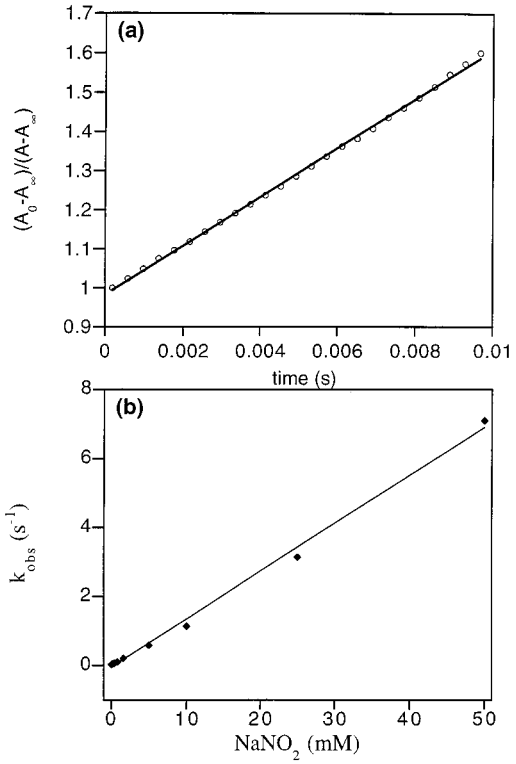

Figure 3. (a) A second-order plot of the stoichiometric reaction between oxoMn(V) intermediate **1** and $NaNO_2$. OxoMn(V) was generated in the first push by mixing 5 μM Mn(III)TMPyP and 5 μM *m*-CPBA, followed by addition of 5 μM $NaNO_2$ in the second push (age time = 0.022 s). The reactions were monitored at 443 nm. The solid line is a linear least-squares fitting of the experimental data ($k = 1.5 \times 10^7$ M^{-1} s^{-1}, $R = 0.9995$). (b) Plot of the pseudo-first-order rates (k_{obsd}) of the oxoMn(IV) (**2**) and $NaNO_2$ reactions vs the $NaNO_2$ concentrations. Each data point is the mean of 3−6 trials (% standard deviation < 4%). OxoMn(IV) was generated in the first push by mixing 5 μM Mn(III)TMPyP and 5 μM HSO_5^-, followed by addition of $NaNO_2$ in the second push (age time = 2 s). The solid line is the linear least-squares fit of the experimental data, which gives a second-order rate constant of 1.4×10^2 M^{-1} s^{-1} ($R = 0.9979$).

(III) was estimated to be 6.5×10^5 M^{-1} s^{-1} (Figure 4b). This very fast, bimolecular oxygen atom transfer indicates that intermediate **1** is a potent and efficient two-electron oxidant.

Two reasonable structures for **1** are a peroxyacid−Mn(III) adduct[10e,h] and the elusive oxoMn(V) complex **1** (Scheme 1).[10f−12] Several lines of evidence support the latter assignment. First, the formation of the epoxide of **3** in the presence of $H_2{}^{18}O$ (95%) led to 35% incorporation of oxygen label from the solvent into the product.[19] This is consistent with the exchange observed by Bernadou *et al.*[16a] for the Mn(III)TMPyP-catalyzed epoxidation of **3** with HSO_5^- and by us for the Mn(III)TMP-catalyzed epoxidation of *cis*-β-methylstyrene in the presence of $H_2{}^{18}O$.[10f] Second, the *same intermediate* **1** could be detected upon oxidation of Mn(III)TMPyP with either HSO_5^- or ClO^-. In these cases, the rates of formation of **1** were slower, 6.9×10^5 and 6.3×10^5 M^{-1} s^{-1}, respectively. Although the reactive intermediate could not be formed to its full extent with these oxidants, a blurring of the isosbestic points was observed between the Mn(III) and oxoMn(IV) Soret maxima consistent with the appearance of **1** (Figure 5a). In both cases, however, an intermediate with the characteristic Soret maximum at *ca.* 441 nm could be observed 1.5 ms after mixing by difference spectroscopy (Figure 5b). Finally, the very fast reduction of **1** by nitrite ion is consistent with the high oxidation potential of water-soluble Mn(IV) porphyrins (>1.15 V) estimated by Bruice[20] and the known oxidation potential of NO_2^- (1.04 V).[21]

The sharp Soret and Q-bands of **1** and the absence of any visible absorbance near 700 nm supports a Mn(V) electronic structure rather than a Mn(IV)porphyrin cation radical (Figure 1). By analogy to the isoelectronic nitridomanganese(V) porphyrin complexes[11] and the few known stable oxoMn(V) complexes,[13,14] the reactive oxoMn(V) porphyrin **1** is expected to be a low-spin, d^2 complex. Accordingly, the high reactivity reported here for **1** for both one-electron and oxygen transfer reactions can be associated more with redox potentials than with unpaired electrons.[22] Specifically, the huge rate difference between the first and second reductions of **1** by nitrite ion fit well with the observation of radical-like reactions of manganese porphyrins. Further, the nitrite-mediated protection of DNA against cleavage by peroxynitrite and manganese porphyrins we have reported[15] can now be more firmly associated with the oxomanganese(V) intermediate as well.

The degree of ^{18}O-exchange observed into the product epoxide is also mechanistically informative. Meunier et al. have

(19) Epoxidation of CBZ was performed in the presence of $H_2{}^{18}O$ (95%). (Detailed reaction conditions and experimental data are available in the Experimental Section.)

(20) (a) Jeon, S.; Bruice, T. C. *Inorg. Chem.* **1992**, *116*, 4843−4848. (b) Kaaret, T. W.; Zhang, G. H.; Bruice, T. C. *J. Am. Chem. Soc.* **1991**, *113*, 4652−4656.

(21) Stanbury, D. M. *Adv. Inorg. Chem.* **1989**, *33*, 69−138.

(22) For a discussion of the oxygenation of toluene by permanganate, see: Gardner, K. A.; Mayer, J. M. *Science* **1995**, *269*, 1849−1851.

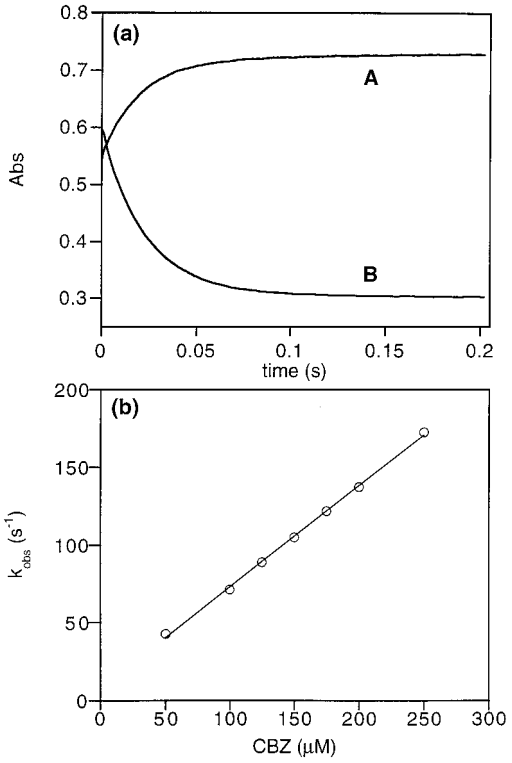

Figure 4. (a) Typical kinetic profiles of the oxoMn(V) intermediate **1** and CBZ reactions in the double-mixing experiments. In the example shown here, the intermediate **1** is about 5 μM and CBZ is 50 μM. The top trace (A) is monitored at 462 nm (the recovery of Mn(III)TMPyP), and the bottom trace (B) is monitored at 443 nm (the decay of **1**). Nonlinear least-squares fitting of these two traces give the same pseudo-first-order rate constants (462 nm, $k_{obsd} = 45.4\ s^{-1}$, $R = 0.9991$; 443 nm, $k_{obsd} = 43.1\ s^{-1}$, $R = 0.9999$). (b) Linear least-squares fitting of the pseudo-first-order rate constants (k_{obsd}) vs CBZ concentrations for the reaction between **1** and CBZ in the double-mixing experiments. Each data point is the mean of 3−5 trials (% standard deviation < 4%). The second-order rate constant is $6.5 \times 10^5\ M^{-1}\ s^{-1}$ ($R = 0.9994$).

Scheme 1[a]

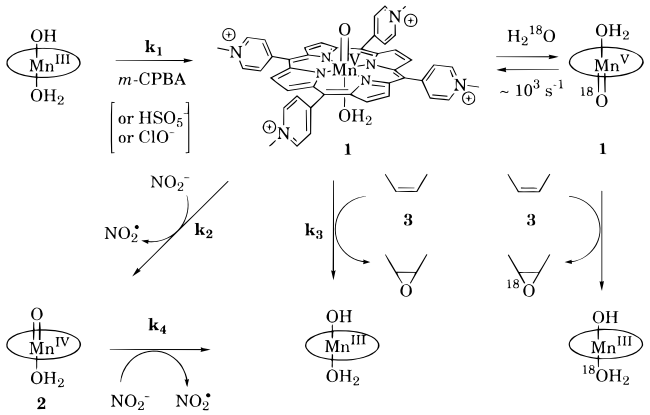

[a] (a) Rate constants: $k_1 = 2.7 \times 10^7\ M^{-1}\ s^{-1}$; $k_2 = 1.5 \times 10^7\ M^{-1}\ s^{-1}$; $k_3 = 6.5 \times 10^5\ M^{-1}\ s^{-1}$; $k_4 = 1.4 \times 10^2\ M^{-1}\ s^{-1}$; ^{18}O-exchange $\approx 10^3\ s^{-1}$. (b) ^{18}O-Incorporation: 35% ^{18}O labeling from the solvent (95% $H_2{}^{18}O$) into the epoxide.

interpreted the maximum 50% incorporation observed with $KHSO_5^-$ and MnTMPyP as the result of an aqua−oxo interconversion via prototropy between those bound ligands.[16] Our results are consistent with this conclusion. Thus, with the absolute rate constant determined here for epoxide formation and the 35% ^{18}O-incorporation into the epoxide, one can estimate the rate of oxo−aqua interchange in the intermediate oxomanganese(V) species **1** ($k_{exchange} \approx 10^3\ s^{-1}$) under these

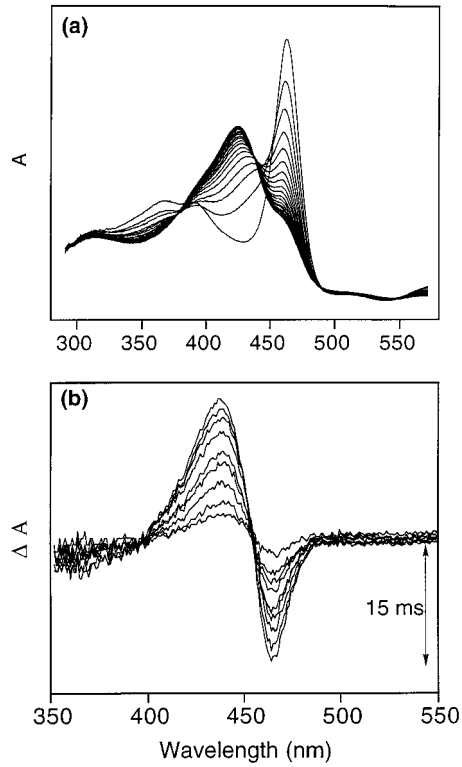

Figure 5. (a) Time-resolved UV−vis spectra for the reaction of 5 μM Mn(III)TMPyP and 5 μM HSO_5^- (100 scans in 1 s, 0.005 s integration time for the photodiode array; full ordinate scale 0.50 OD; every fifth scan shown). (b) Difference spectra define for the first 15 ms of the same reaction (100 scans in 150 ms, 0.0015 s integration time for the photodiode array; full ordinate scale 0.10 OD; difference spectrum = spectrum(t) − spectrum(0)).

conditions. Significantly, water exchange between the bulk solvent and the oxo species must be *slower* than that. The known inhibition of ^{18}O-exchange into substrate olefins from oxoMn(V) intermediates by added pyridine[10f] supports this view. Accordingly, the limited degree of ^{18}O-exchange observed with some metalloporphyrin catalysts[23] cannot be used to exclude an oxo intermediate since the relative rates of oxygen exchange and oxygen transfer to the substrate may not be appropriate to reveal exchange. Further, a *bona fide* metal−oxo intermediate can be anticipated with confidence in those cases in which ^{18}O-exchange is observed with a nonexchanging oxidant such as a peroxyacid.[10b,f,16a]

We have shown that a reactive intermediate (**1**) can be produced from the reaction of Mn(III)TMPyP with a variety of oxidants (*m*-CPBA, HSO_5^-, OCl^-) under ambient, catalytic conditions. The reactions observed for **1** reported are most consistent with an oxomanganese(V) formulation for this species. The success of this rapid kinetic approach to detecting the individual steps in oxidative catalysis suggests its application to other elusive intermediates in these processes.

Experimental Section

Materials. Mn(III)TMPyP was purchased from Mid-Century Chemical. Potassium peroxymonosulfate, 3-chloroperoxybenzoic acid (*m*-CPBA), sodium hypochlorite, sodium nitrite, and carbamazepine were obtained from Aldrich. $H_2{}^{18}O$ was purchased from Cambridge Isotope Laboratories, Inc. Anhydrous monosodium phosphate and disodium phosphate were obtained from Sigma. All the solvents are analytical grade. Water used in all the experiments was distilled and deionized (Millipore, Milli-Q).

(23) Nam, W.; Valentine, J. S. *J. Am. Chem. Soc.* **1993**, *115*, 1772−1778.

Time-Resolved Visible Spectra. All the time-resolved visible spectra were recorded on a HI-TECH SF-61 DX2 stopped-flow spectrophotometer using the photodiode array fast-scan mode. The spectral resolution was about 1 nm. Stoichiometric reactions between Mn(III)TMPyP and oxidants (*m*-CPBA, HSO_5^-, ClO^-) were performed by single mixing, and the concentrations presented were the final concentrations after mixing. The porphyrin solutions were buffered with 50 mM sodium phosphate, pH 7.4. The same reactions were also performed in the presence of $NaNO_2$ and CBZ.

Reaction Kinetics. Reaction kinetic profiles were collected in the photomultiplier mode on the HI-TECH SF-61 DX2 stopped-flow spectrophotometer using single- or double-mixing modes. Mn(III)-TMPyP, oxoMn(V) (**1**), and oxoMn(IV) (**2**) were monitored at 462, 443, and 428 nm, respectively. Reactions of Mn(III)TMPyP with *m*-CPBA were stoichiometric and those with HSO_5^- or ClO^- were pseudo-first-order in oxidant concentrations.

The reduction rates of **1** and **2** by $NaNO_2$ were measured directly by performing double-mixing experiments: the intermediates were fully generated during the first mixing step and then the $NaNO_2$ was added in the second mixing step. The reaction of **1** and $NaNO_2$ was analyzed as a second-order reaction. The reactions of **2** and $NaNO_2$ were performed under pseudo-first-order conditions in nitrite concentrations. The reaction rate of **1** and CBZ to afford Mn(III) and carbamazepine-oxide was similarly estimated by double-mixing experiments.

HPLC Analysis of the Epoxidation Products of CBZ. All reactions were performed according to the following procedures: Carbamazepine (1.2 mM) and *m*-CPBA (5 mM) stock solutions were prepared by dissolving the compounds in minimum amount of methanol and then dispersing into 50 mM pH 7.4 phosphate buffer and deionized water, respectively. Into a 940 μL reaction mixture of 50 nmol of Mn(III)TMPyP and 520 nmol of CBZ in 50 mM pH 7.4 phosphate buffer, 300 nmol of *m*-CPBA was added in six aliquots of 50 nmol (10 μL) each at 2 min intervals. A similar reaction in the absence of porphyrin catalyst was used as a control. Nitrite inhibition of the epoxidation reaction was carried out similarly as described above, except in the presence of 600 μM $NaNO_2$. Quantitative analyses of the reaction products were performed by HPLC. CBZ and its epoxide derivative were separated on a Waters Delta PAK 5 μm C18 300 Å column eluted by a mixture of methanol and 2 mM NaH_2PO_4, 45:55 (v/v), with retention times of 8.2 and 4.0 min, respectively. Concentrations were determined on the corresponding calibration curves of CBZ and the authentic carbamazepine-oxide. Under the above conditions, the conversion (based on oxidant) is 35% and the yield of epoxide is 93%. In the presence of nitrite ion, less than 3% of the epoxide was found.

^{18}O Incorporation into the Carbamazepine Oxide. Epoxidation of CBZ in the presence of $H_2{}^{18}O$ (95%) was performed according to the following procedures: Mn(III)TMPyP (7.7 mM), CBZ (78.8 mM), and *m*-CPBA (50 mM) were introduced into 50 mM pH 7.4 phosphate buffer ($H_2{}^{18}O$) as methanol solutions. Into a reaction mixture of 50 nmol of Mn(III)TMPyP and 1 μmol of CBZ, 1.25 μmol *m*-CPBA was added in five aliquots of 250 nmol (5 μL) each at 2 min intervals. Then, another 50 nmol Mn(III)TMPyP was added to the reaction mixture and five more aliquots of 250 nmol *m*-CPBA were added (final volume 1 mL). The reaction mixture was extracted with 1 mL of CH_2Cl_2 twice, and then the organic solvent was evaporated under vacuum to dryness. Samples were diluted with CH_2Cl_2 before MS analyses. Electronic impact mass spectra revealed a stable fragment ($M^{+\bullet} - CH_3NO$) of carbamazepine oxide with the following peak intensities (% base area) in the ^{16}O-controls: *m*/*z* 206 (10.7), 207 (100), 208 (17), 209 (7.4), 210 (2.1), and 211 (1.6). In the ^{18}O-exchange samples, the fragment peak intensities were *m*/*z* 206 (11.8), 207 (100), 208 (23.7), 209 (65.9), 210 (11.7), and 211 (6.2). Therefore, the percentage of carbamazepine [^{18}O]oxide is 37%, which was further confirmed by both the weaker molecular peak intensities at *m*/*z* 252 (100.00), 254 (49.56) (35% ^{18}O incorporation) and the time-dependent TIC at *m*/*z* 252 (100) and 254 (60) (37% ^{18}O incorporation). The authentic [^{16}O]epoxide did not exchange with $H_2{}^{18}O$.

Acknowledgment. Support of this research by the National Institutes of Health (GM36928), the National Science Foundation for the purchase of 500 and 600 MHz NMR spectrometers, and Princeton University for the purchase of a stopped-flow spectrophotometer are gratefully acknowledged.

JA962605U